A Nano-Platform for in situ Investigations of Ovarian Follicles

Jean M. Feugang (j.feugang@msstate.edu)
Mississippi State University https://orcid.org/0000-0002-1376-5059
Ghassan Ishak
Southern Illinois University Carbondale
Matthew Eggert
Auburn University
Robert Arnold
Auburn University
Scott Willard
Mississippi State University
Peter Ryan
Mississippi State University
Eduardo Gastal
Southern Illinois University Carbondale

Research

Keywords: Liposome vesicles, Molecular imaging, Nanoparticles, Targeted drug delivery, Ovarian follicles, Intrafollicular injection, Livestock, Assisted reproductive technology

Posted Date: September 22nd, 2020

DOI: https://doi.org/10.21203/rs.3.rs-78063/v1

A nano-platform for *in situ* investigations of ovarian follicles

J M Feugang[1,*], G M Ishak[2,3], M Eggert[4], R D Arnold[4], S T Willard[1], P L Ryan[1], E L Gastal[3]

[1] *Department of Animal and Dairy Sciences, Mississippi State University, Mississippi State, MS, USA*

[2] *Department of Surgery and Obstetrics, College of Veterinary Medicine, University of Baghdad, Baghdad, Iraq*

[3] *Department of Animal Science, Food and Nutrition, Southern Illinois University, Carbondale, Illinois, USA*

[4] *Department of Drug Discovery and Development, Harrison School of Pharmacy, Auburn University, Auburn, AL, USA*

[*] **Corresponding author**: Jean M. Feugang, Department of Animal and Dairy Sciences, Mississippi State University, Mississippi State, MS, USA. 335 Wise Center, PO Box 9815 Mississippi State, MS 39762. Tel. (662) 325-7567; FAX: (662) 325-8873 E-mail: j.feugang@msstate.edu

Abstract

Background: Despite the growing array of assisted reproductive techniques, there is still a lack of rapid, non-cytotoxic, and minimally invasive *in situ* approaches for further enhancements through cell targeting. Here we synthesized clinically relevant liposome nanoparticles for real-time cellular targeting and drug (doxorubicin) delivery, using pigs and mares as animal models. In Experiment 1, fluorescently labeled and doxorubicin-loaded (without fluorescent probe) liposomes were injected in cultured pig ovarian follicles to assess plasma membrane binding and intracellular doxorubicin delivery. In Experiment 2, fluorescent liposomes were *in vivo* injected into small and large ovarian follicles of living mares to assess their binding capability to follicular cells. Twenty-four hours post-injection, all cultured pig follicles were collected while mare samples (i.e., follicle wall fragments, granulosa cells and follicular fluids) were harvested through follicle wall biopsy (FWB), and follicle aspiration and flushing techniques using transvaginal ultrasound-guided approach.

Results: All injected follicles were healthy and samples were subjected to fluorescence imaging before and after fixation. Findings revealed successful intrafollicular migration and binding of liposomes to all follicle cell layers (granulosa, theca interna, and theca externa) regardless of the follicle size. The intracellular delivery of doxorubicin was confirmed with the staining of nuclei of follicle cells.

Conclusions: This study demonstrates the promising combination of the FWB technique and nanotechnology tools for real-time monitoring of intrafollicular treatment, follicular health and oocyte development, which in turn has the potential to help understand the mechanisms of ovulatory dysfunction and to select high-quatity oocytes for assisted reproduction techniques.

Keywords: Liposome vesicles, Molecular imaging, Nanoparticles, Targeted drug delivery, Ovarian follicles, Intrafollicular injection, Livestock, Assisted reproductive technology

Background

The current efforts to overcome fertility problems through assisted reproductive technologies (ARTs) are still unsatisfactory because of the insufficient maturation of the oocytes and/or the existing follicular diseases [1-6]. Furthermore, the ability to assess the quality of the oocytes mainly, if not only, through *in vitro* manipulations constitutes a serious limitation [7, 8]. Hence, the development of novel methods for *in situ* assessment of oocyte quality and local (versus systemic) treatments of unhealthy follicles prior to the retrieval of enclosed oocytes would be of great interest.

Challenges related to female fertility treatments need the investigation of various methodologies. For example, the routine systemic drug injections (i.e., exogenous gonadotropins) for controlled ovarian hyperstimulation (COH) is showing increased evidence of detrimental effects on oogenesis, embryo quality, and endometrial receptivity [9-12]. Hence, intrafollicular injection, which has been applied in large animals (e.g., cow and mare) with relative success [4, 13], may become a viable alternative to COH, and the recent advances in nanotechnology and assisted reproduction tools are likely to boost the outcomes of intrafollicular treatments.

At present, the primary use of “naked” biomolecules, without a carrier, for intrafollicular injection has drastically limited their potential to gain mechanistic insights related to follicle

growth and oocyte maturation. Interestingly, the recent detection of extracellular membrane microvesicles in equine [14], human [15], and bovine [16] follicular fluid (FF) and their roles as delivery carriers of biomolecules (e.g., lipids, proteins, RNAs, and miRNA) enabling intercellular communications have prompted new interest in the use of liposome nanoparticles for intrafollicular injections [17-19]. Liposomes are clinically relevant carbon-based nanoparticles shaped like spherical vesicles constituted of phospholipid bilayers providing biocompatibility, biodegradability, and low toxicity to cells [20]. These nanoparticles have been used as effective carriers for controlled and rapid deliveries of various hydrophilic and hydrophobic molecules to specific biological sites, with indubitable benefits during *in vivo* and *in vitro* applications [21, 22]. For fertility treatments, several drugs, including biomolecules that are found in the FF [23-27], can be loaded into liposomes for intrafollicular injections.

Following intrafollicular injections, the minimally invasive *in vivo* Follicle Wall Biopsy (FWB) technique is a recently improved methodology for assisted reproduction allowing for simultaneous sampling of the follicle environment (FF, granulosa, theca interna and externa cells) for *ex vivo* examinations. Most importantly, the FWB technique is performed on living mares without affecting their fertility, ovarian function, or the FF composition, therefore providing an excellent cocktail for biomarkers research and clinical purposes [28, 29]. Its combination with the encapsulated liposomes for intrafollicular deliveries can be highly effective for a more in-depth understanding of the molecular mechanisms governing follicle growth and oocyte maturation.

In the current study, fluorescent and non-fluorescent unilamellar liposome vesicle nanoparticles were synthesized. Fluorescence was used for the visualization of the tissular

distribution, and non-fluorescent liposomes were loaded with doxorubicin to assess intercellular delivery. The effectiveness of the liposome nanoparticles in binding the plasma membrane of follicle cells and delivering doxorubicin was tested *in vitro* with cultured pig ovarian follicles (*ex situ - Experiment 1*). Thereafter, as the first step to implement *in situ* fertility treatments and deep-tissue imaging, the binding capability of liposomes in living animals was tested using intact equine ovarian follicles (*in situ – Experiment 2*).

Results

Characterization of synthesized liposome nanoparticles

The formulated liposome characterization in Tris buffer pH 7.5 indicated a z-average nanoparticle diameter of 124.7 nm (PDI = 0.106), a number average diameter of 87.7 ± 27.5 nm (Fig. 1A), and a zeta potential mean of –22.9 ± 9.51 mV (Fig. 1B). The addition of 1% DiI to the formulated fluorescent liposomes led to a final hydrodynamic average diameter of 109.9 ± 17.5 nm, while the TEM imaging indicated a dry average diameter of 21.3 ± 4.5 nm (± SEM), calculated for thirty random liposomes (Fig. 1A- Insert). For this study, three independent liposomes were formulated with high fluorescence intensity ($1.9x10^{11}$ ± $8.x10^{9}$ radiance; Fig. 2A). Their mixture and dilution with PBS resulted in the working liposome solution of 23.1 µM DiI dye with fluorescence intensity of $6.5x\ 10^{10}$ radiance (IVIS imaging; Fig. 2B).

Experiment 1. Assessment of liposome binding and doxorubicin delivery in cultured porcine follicles

IVIS imaging of dissected porcine antral follicles

Decreasing fluorescence signals with PBS-injected liposomes (auto fluorescence; upper follicle series) when compared to those injected with fluorescence liposomes (middle follicle series) or liposomal encapsulated doxorubicin (lower follicle series) can be seen in Figure 3A. Data quantification confirmed higher ($P < 0.05$) fluorescence signals of both liposome- ($1.35 \times 10^9 \pm 5.31 \times 10^8$) and doxorubicin-injected follicles ($1.82 \times 10^9 \pm 8.38 \times 10^8$) and radiant efficiency, when compared with the PBS-injected group ($3.93 \times 10^8 \pm 1.53 \times 10^8$; Figure 3B); however, the fluorescence signals in both liposome and doxorubicin groups were comparable ($P > 0.05$).

Microscopy imaging of liposome binding and doxorubicin delivery

Imaging was performed on follicle wall sections on microscope slides. Autofluorescence or low/background fluorescence can be observed in sections of follicles injected with PBS (Fig. 4A). In contrast, the highest fluorescence intensity observed in the plasma membranes of follicle wall cells confirmed the liposome binding (Fig. 4B). The successful binding of doxorubicin-loaded liposomes to cellular plasma membranes and the delivery of doxorubicin (10 µg/follicle) to the nucleus (red dots) of various cell types of the follicle wall (Fig. 4C) were observed; and highlights the colocalization of red (doxorubicin) and blue staining (DAPI) within the nuclei can be seen in Figure 4D- Insert.

Experiment 2. *In vivo* liposome binding in living mares and *ex vivo* imaging

A total of 22 growing and healthy follicles of nine mares (2-3 follicles/mare) were successfully injected with 130 µl of fluorescent liposomes working stock solution.

IVIS imaging of FWB

All FWB samples were of comparable areas (3.5 ± 0.3 mm^2), and those of liposome-injected follicles exhibited fluorescence intensities above background (Control; 6.7 $x10^8$ ± 1.44 $x10^7$ radiant efficiency; Fig. 5A). The FWB derived from both small and large follicles had comparable fluorescence intensities (1.74 $x10^9$ ± 7.6 $x10^8$ and 1.98 $x10^9$ ± 3.4 $x10^8$ radiant efficiency, respectively, $P > 0.05$; Fig. 5B). *In vitro* labeling of FWB with an equivalent amount of liposomes (130 µl = 1.2 nmoles; 60 min at 37°C) led to higher (3.92 $x10^9$ ± 1.11 $x10^8$ radiant efficiency, $P < 10^{-4}$) fluorescence intensity than that of other groups (Fig. 5B).

IVIS imaging of intrafollicular fluid

The FF of both non-injected (control) and PBS-injected follicles emitted low fluorescence intensities that were considered background and subtracted from those of FF harvested from small (Fig. 6A) and large (Fig. 6B) follicles injected with liposomes ($P < 10^{-4}$; Fig. 6C). Data quantification shows higher fluorescence intensity from small follicles' FF (2.95 $x10^9$ ± 9.65 $x10^8$ radiant efficiency) than their large counterparts (8.53 $x10^8$ ± 0.98 $x10^8$ radiant efficiency).

IVIS imaging of granulosa cells (GC)

Fluorescence signals of GC harvested from both small and large follicles were above background (non-injected or control follicles: 7.4 $x10^8$ ± 1.23 $x10^7$ radiant efficiency, $P < 10^{-5}$; Fig. 7A). Large follicles' GC produced higher fluorescence than that of small follicles (1.61 $x10^9$ ± 6.83 $x10^7$ *vs.* 9.12 $x10^8$ ± 1.67 $x10^7$ radiant efficiency, $P < 0.05$; Fig. 7B).

Confocal microscope fluorescence imaging of FWB samples and flushed granulosa cells

The uniform staining of cell nuclei with DAPI (blue) revealed the good health status of harvested samples. Follicles injected with PBS did not show any fluorescence (green staining) corresponding to the presence of liposomes (Fig. 8A). In contrast, follicles injected with liposomes displayed green fluorescence staining within the plasma membrane of the follicle wall cells (Fig. 8B). The insert in Figure 8B highlights the fluorescence signal on the plasma membrane surrounding the blue staining of the nuclei; this observation is confirmed with the images of flushed mural granulosa cells showing stronger fluorescence signals within the plasma membrane (Fig. 8C,D). The smeared fluorescence signals seen in Figure 8C,D on the tissues surrounding the GC correspond to liposomes bound/trapped within the extracellular matrix.

Discussion

Many factors, such as the physiological conditions of animals and the available technologies, are prone to influence assisted reproduction outcomes in animals. Here we examined a clinically relevant liposome vesicle nanoparticle as a potentially powerful, non-invasive diagnostic and therapeutic agent for future assessment and treatment of ovarian follicles prior to oocyte recovery. Monovular (mare) and polyovular (pig) species were used to demonstrate the likely application of our proposed technological approach for *in situ* follicle investigation and improvement of female fertility.

Herein, the sizes of the synthesized liposomes were comparable to those in previous reports [20, 30, 31], while the injected volumes (5 µl in pigs and 200 µl in mares) and incubation time (24 h) were lesser or equal to those reported in previous studies [4, 32]. Hence, the absence of

morphological changes in both equine and porcine ovarian follicles' structures following intrafollicular injections was highly important, with the prospect of performing local deliveries (i.e., intrauterine or intrafollicular) of molecules at minimal effective doses to reach the targeted cells during ovarian follicle treatments [33]. These minimal effective doses following local injections (*vs.* systemic treatments) were demonstrated in mares [34] and cows [13] using PGF2α (≤ 0.1 mg *vs.* up to 50-fold greater) and hCG (1.0 IU *vs.* up to 1000-fold greater), respectively. The ability to by-pass the systemic route (i.e., intramuscular or intravenous) and avoid the dilution with the blood-stream through local injections of growing antral follicles permits the study of the direct effects of biocompounds (insulin-like growth factor 1, eCG, and PGF2α) during folliculogenesis [4, 34, 35]. These studies highlight the promising interest in intrafollicular treatments in animal production and veterinary medicine; however, most related studies use "naked" (devoid of additional carriers) biomolecules whose ability to cross cell membranes and short lifespan may be jeopardized during long incubations or journeys.

Interestingly, the current progress in nanotechnology is increasing the popularity of nanoparticles in biomedicine. These nanoparticles possess specific properties (e.g., size-dependent synthesis, bright and broad-spectrum fluorescence, biocompatibility and bioconjugation capability) that can be exploited for further investigation and improvement of reproductive outcomes [22, 32, 36]. In the present study, we used liposomes shaped like extracellular membrane microvesicles (EVs), which are nano- and micro-size vesicles naturally released from cells to mediate a new type of cell-to-cell communication through passive interactions [17, 18, 37]. Likewise, liposomes can interact and fuse with somatic cells (e.g., MCF-7 breast cancer cells) within approximately five minutes post-incubation [38]. In the

197 present study, the pig model allowed the (IVIS) imaging of the full and intact follicle, indicating
198 the possibility for *in situ* non-invasive monitoring of folliculogenesis through molecular imaging
199 of key biological processes. With the existing fluorescence spectrum of hydrophobic dyes, it is
200 reasonable to anticipate the formulation of specific labeled liposomes for multiplex molecular
201 imaging for real-time examinations of various follicular phenomena related to aging, ovarian
202 cyclicity (cycling *vs.* anestrous phase), structural variations (antral follicles *vs.* corpus luteum),
203 reproductive phases (estrous *vs.* diestrous), and health (follicle diseases). Understanding of them
204 may have beneficial implications for women, who are known to share many reproductive
205 similarities with mares [39].
206 The present study highlights the advantage of combining nanotechnology with granulosa cell
207 aspiration and *in vivo* FWB techniques to provide more insights into the intrafollicular
208 microenvironment. Recently, the FWB technique was validated for simultaneous collections of
209 follicle wall fragments and FF samples from the same living mare [28, 29]. Here, we first
210 observed that the expected unidirectionality of liposome binding, from the follicular antrum to
211 the theca externa, leading to lower fluorescence intensity of *in situ* labeled biopsies contrasted
212 with the likely multidirectional binding during *ex situ* labeling; consequently, all follicle cell
213 types simultaneously interacted with the liposomes *ex situ* to generate stronger fluorescence
214 signals. Second, the higher fluorescence of FFs in small follicles was indicative of the low
215 abundance of cells capable of uptaking liposomes. And third, the high abundance of cells in large
216 follicles permitted the binding of more liposomes, leading to reduced unbound fluorescent
217 liposomes in the corresponding FFs. Nonetheless, fluorescence intensity variations between

samples certainly corresponded to the possible losses of liposomes during injections, while the higher fluorescence of large follicles' granulosa cells was attributed to their greater density.

The random and passive characteristics of injected liposomes to fuse with follicular cells' membranes makes them suitable for intracellular deliveries. Indeed, liposomes are among the numerous carriers with efficient intracellular delivery of cargo of molecules such as proteins, nucleic acids, metabolites, and even drugs [14, 17, 18, 36, 38]. Our findings revealed the effective internalization of doxorubicin with its binding to the cell nucleus of all follicle cell types, demonstrating the far-reaching capacity of the proposed injection route.

Conclusions

The current study demonstrates 1) the combination of FWB technique and nanotechnology tools as a promising approach for potential local treatments of ovarian follicle diseases and enhancement of reproductive performance; 2) the possibility for deep-tissue (plain or targeted) imaging using fluorescent-labeled liposomes for *in situ* tracking of molecular and/or cellular processes throughout the antral follicle growth; and 3) the possible use of a formulated liposome carrier in both mono- and polyovulator animals as well as in living large animals. We believe the proposed methodology is likely to support future intrafollicular attempts to promote follicle and/or oocyte growth and to develop treatments to address follicle diseases such as luteinized unruptured follicle in mares and, potentially, in women as well [5, 40].

Methods

Chemical and reagents

Phospholipid, DPPC (1, 2-dipalmitoyl-sn-glycero-3-phosphocholine) was purchased from Avanti Polar Lipids, Inc. (Alabaster, Alabama, USA). Ultrapure grade cholesterol was obtained from Amresco, Inc. (Solon, Ohio, USA). Lipophilic probes, 1, 1'-dioctadecyl-3, 3, 3', 3'-tetramethylindocarbocyanine perchlorate (DiIC18(3) or DiI) and 3,3'-dioctadecyloxacarbocyanine perchlorate (DiOC18(3) or DiO), were acquired from Biotium, Inc. (Hayward, California, USA). Any additional reagents, chemicals, or solvents of necessary molecular biology or analytical grade were obtained through commercial sources.

Liposome nanoparticle preparation and characterization

Fluorescence liposome formulation. Pegylated liposomes were prepared as previously described [41, 42]. Briefly, formulations were generated according to a ratio of 10 µmol DPPC, 5 µmol cholesterol, and 100 nmol of the fluorescent lipophilic probe, DiI (~1 mol % of lipid membrane), per milliliter of dispersant. The lipids and probe, dissolved in chloroform, were mixed and then dried under a rotary vacuum via a Buchi Rotavapor r-200 (Postlfach, Switzerland) to create a thin film. Subsequently, films were hydrated in an isotonic solution of either 10% (w/v) sucrose or phosphate-buffered saline to yield 10 µmol phospholipid/mL. Liposomes underwent seven freeze/thaw cycles via liquid nitrogen and a 60^{o}C water-bath above lipid phase transition temperature as a means to eliminate additional membrane layers. Formulations were then extruded using a Lipex extruder (Northern Lipids Inc., Burnaby, British Columbia, Canada) under high pressure through double-stacked laser etched polycarbonate 80 nm filters (GE Osmonics, Trevose, Pennsylvania, USA) at heated conditions again above DPPC's phase transition temperature (T_c = 41^{o}C) for seven times before stabilizing the lipid membranes using

an ice-bath for 10 min. Afterward, the liposome dispersions were dialyzed with a 12−14 kDa SpectraPor Dialysis membranes against fresh isotonic solution as used in hydration for a period of 1, 4, and 16 hours at 4°C to remove any non-membrane associated probe. Liposomes were sterilized by terminal filtration (0.22 µm filter) and stored in a sterile glass container under nitrogen atmosphere at 4°C, protected from light, and used within 3 weeks of preparation. Lipid concentration was determined for all formulations using an inorganic phosphate assay [43]. Thereafter, the dispersion was diluted to 10 µmol/ml (10 mM), and average stock solutions of liposome nanoparticles (9.24 ± 0.72 µmol/ml or 9.24 mM) were constituted and stored at 4°C for experiments. The DiI lipophilic probe fluoresced at 570 nm following a 480 nm wavelength excitation.

Doxorubicin-loaded liposome formulation. A nonfluorescent pegylated liposomal was formulated by Avanti Polar Lipids, Inc. (Alabaster, Alabama, USA) and used to encapsulate the naturally fluorescing doxorubicin (Dox-NP; referenced maxima Ex/Em of 480nm/590nm). All samples were stored at 4°C for experiments.

High-Resolution Transmission Electron Microscopy and Fluorescence imaging. A subset of synthesized liposomes was visualized under a high-resolution transmission electron microscope (HR-TEM-2100, 200 kV) with Gatan Orius 832 camera (JEOL; Peabody, Massachusetts, USA), while another subset was subjected to non-invasive and real-time fluorescence imaging using the In Vivo Imaging System 200, Lumina XRMS Series III system (IVIS; PerkinElmer; Waltham, Massachusetts, USA).

Experiment 1. Porcine antral follicle culture and intrafollicular liposome injection

Porcine ovaries were harvested in a pre-warmed 0.9% NaCl solution at a local slaughterhouse and transported immediately to the laboratory. Visible and morphologically normal antral follicles (4–8 mm in diameter) were dissected and randomly distributed in a set of 24-well tissue culture plates (3–4 follicles/well); subsequently, the tissue culture plates were placed in a 5% CO_2 incubator as previously reported [32]. After 24 h of culture at 37^{o}C in a humidified environment, follicles were microinjected using FemtoJet microinjection system (Eppendorf; Hauppauge, New York, USA) with 5 µl of Phosphate-Buffered Saline solution (PBS) or 46 nmol of fluorescent liposomes. Thereafter, injected follicles were returned to their respective culture wells with half of the medium renewed (1.5 ml of NCSU-23 based medium) and re-incubated for an additional day of culture. A subset of non-injected follicles was kept in culture to serve as controls for auto-fluorescence. Following culture, follicles were carefully removed from culture wells and washed twice in PBS solution prior to non-invasive IVIS fluorescence imaging. Thereafter, follicles were processed for standard histology and fluorescence microscopic imaging.

Experiment 2. *In vivo* liposome binding tests in living mares

Animals, ultrasonography examination, and intrafollicular fluorescent liposome injection.

Nine nonlactating and cycling Quarter Horse breed mares, 8−14 years old, and weighing 400−600 Kg were used during the ovulatory season. Mares were kept under natural light in pasture and were maintained with free access to water and trace-mineralized salt. Ovarian follicle

306 tracking was performed daily starting on day 10 of the estrous cycle (day 0 = ovulation) until
307 follicles reached the designated diameter. Ultrasonographic follicle tracking was carried out
308 using a duplex color Doppler ultrasound machine (Aloka SSD-3500; Hitachi Aloka Medical
309 America, Inc., Wallingford, CT, USA) equipped with a finger-mounted 3.5−10 MHz convex-
310 array transducer (UST-995-7.5). After identification and mapping of small (15−23 mm; n = 12)
311 and large (24−30 mm; n = 10) follicles that showed continuous growth for a minimum of three
312 consecutive days, fluorescent liposome nanoparticles (130 µl; 23.1 µM or 1.2 nmol) were
313 injected into each growing follicle using a double-channel injection system as previously
314 described [4, 44]. All mares (n = 9) were used for the injection of 22 follicles (12 small and 10
315 large), corresponding to 2−3 follicles per mare. One small and one large noninjected follicle
316 served as experimental controls. After follicle injections, all mares were released to the pasture
317 for 24 h. Thereafter, all samples (FWB, FF, and isolated granulosa cells) were collected for
318 analyses.
319
320 ***Mare antral follicle wall biopsy and follicular fluid collection.*** A novel FWB technique recently
321 developed in our lab [29] was used to simultaneously harvest FWB and FF from PBS- and
322 liposome-injected follicles (7 small and 7 large) and one non-injected (control) follicle. This
323 technique uses an endoscopic biopsy forceps (5 FR gauge, 60 cm, Karl Storz, Berlin, Germany)
324 located inside a 12 G needle/cannula and mounted on a 5−10 MHz transvaginal ultrasound-
325 guided convex array transducer (Aloka UST-987-7.5). The FWB samples measured
326 approximately 3.5 ± 0.3 mm^2 in area, as previously reported [29]. Immediately after FWB
327 harvesting, FF was collected while the needle was still inside the follicle. Intrafollicular fluid

328 samples were centrifuged at 4ºC (1,500 *g* for 10 min), and the supernatant of each FF sample
329 was stored in light safe black Eppendorf tubes at 4ºC.
330
331 ***In situ collection of equine granulosa cells.*** The remaining injected (6 small and 5 large) and
332 non-injected (1) follicles were flushed with 120−150 ml of pre-warmed (38ºC) Vigro complete
333 embryo flush with BSA solution (Bioniche; Pullman, WA, USA) containing 2 IU/ml heparin
334 (H3149, Sigma-Aldrich; Saint-Louis, MO, USA), and granulosa cells were retrieved. Thereafter,
335 flushing fluid was filtered through a 70-μm cell strainer, and concentrated granulosa cells were
336 washed out from the strainer with PBS into a petri dish and transferred into light safe black
337 Eppendorf tubes. After centrifugation (800 g for 10 min) at 4ºC, the supernatant was discarded,
338 and the pelleted granulosa cells were kept at 4ºC until fluorescence imaging.
339
340 **Fluorescence microscopic imaging**
341 All samples were imaged within a week post-collection.
342
343 ***IVIS imaging.*** Equine FF, granulosa cells, and FWB samples, as well as cultured porcine
344 follicles, were collected and subjected to non-invasive and real-time fluorescence imaging using
345 the IVIS imaging system (PerkinElmer; Waltham, Massachusetts, USA).
346
347 ***Fluorescence imaging***. Following IVIS imaging, porcine follicles and equine FWB samples
348 were fixed in 10% formalin solution for standard histology processing, generating 4−6 μm
349 sample sections per slide. Fixed equine granulosa cells were spread on histology slides, air-dried,

immersed with a DAPI-contained mounting medium, and covered by a cover-slip. Slides were imaged with an epifluorescence microscope (EVOS FL-Auto Cell Imaging System, Thermo Fisher Scientific Inc., Waltham, MA, USA) or a confocal laser scanning with an Inverted microscope (Axiovert 200M) coupled with Zeiss ZEN digital imaging software (Carl Zeiss AG; Oberkochen, Germany).

Statistical analyses

All statistical analyses were performed using SPSS v22 software. The Student's t-test and One-way Analysis of Variance (ANOVA) were used, wherever appropriate, to compare the difference between groups (control, small and large follicles). The threshold of significance was set for p-values less or equal to 0.05. All data are expressed as mean ± SEM.

List of abbreviations

PBS: Phosphate-buffered saline; FWB: Follicle Wall Biopsy; DAPI: 4′,6-diamidino-2-phenylindole; GC: Granulosa Cells; FF: Follicular Fluid; IVIS: In Vivo Imaging System; DiI: 1,1'-Dioctadecyl-3,3,3',3'-Tetramethylindocarbocyanine Perchlorate; SPSS: Statistical Product and Service Solutions.

Ethics approval and consent to participate

All experimental procedures were performed according to the United States Government Principles for the Utilization and Care of Vertebrate Animals Used in Testing, Research and Training (grants.nih.gov/grants/olaw/references/phspol.htm). The use of animals and procedures

were approved by the Institutional Animal Care and Use Committee of Southern Illinois University.

Consent for publication

Not applicable.

Availability of data and materials

Data sharing is not applicable to this article as no datasets were generated or analyzed during the current study.

Competing interests

The authors declare that they have no competing interests.

Funding

This material is based upon work that is supported by the National Institute of Food and Agriculture, U.S. Department of Agriculture, Hatch project accession number 1016077 and Multistate number W4171. Additional funds for research and APC were provided by the USDA-ARS Biophotonics (58-6402-3-018).

Authors' contributions

JMF and ELG conceptualized the study; ME and RDA synthesized and characterized the liposome nanoparticles; JMF, GMI, and ELG performed the experiments and collected data;

JMF, GMI, ME, and ELG analyzed the data and wrote the first draft of the manuscript; RDA, PLR and STW contributed to the conceptualization and data interpretation. All authors read and approved the final manuscript.

Acknowlegdments

The authors thank Dr. Melba Gastal and Gabriel Dutra for their technical assistance.

References

1. Motlik J, Crozet N, Fulka J: **Meiotic competence in vitro of pig oocytes isolated from early antral follicles.** *Reproduction* 1984, **72:**323-328.
2. Gilchrist RB, Thompson JG: **Oocyte maturation: emerging concepts and technologies to improve developmental potential in vitro.** *Theriogenology* 2007, **67:**6-15.
3. Feugang JM, Camargo-RodrÃ-guez O, Memili E: **Culture systems for bovine embryos.** *Livestock Science* 2009, **121:**141-149.
4. Gastal EL, Kot K, Ginther OJ: **Ultrasound-guided intrafollicular treatment in mares.** *Theriogenology* 1995, **44:**1027-1037.
5. Bashir S, Gastal MO, Tazawa SP, Tarso S, Hales DB, Cuervo-Arango J, Baerwald AR, Gastal EL: **The mare as a model for luteinized unruptured follicle syndrome: intrafollicular endocrine milieu.** *Reproduction* 2016, **151:**271-283.
6. Hinrichs K: **Production of embryos by assisted reproduction in the horse.** *Theriogenology* 1998, **49:**13-21.
7. Lonergan P, Fair T: **Maturation of Oocytes in Vitro.** *Annual Review of Animal Biosciences* 2016, **4:**255-268.
8. Hansen PJ: **Implications of Assisted Reproductive Technologies for Pregnancy Outcomes in Mammals.** *Annual Review of Animal Biosciences* 2020, **8:**395-413.
9. Horcajadas JA, Mínguez P, Dopazo J, Esteban FJ, Domínguez F, Giudice LC, Pellicer A, Simon C: **Controlled ovarian stimulation induces a functional genomic delay of the endometrium with potential clinical implications.** *The Journal of Clinical Endocrinology & Metabolism* 2008, **93:**4500-4510.

10. Haouzi D, Assou S, Dechanet C, Anahory T, Dechaud H, De Vos J, Hamamah S: **Controlled ovarian hyperstimulation for in vitro fertilization alters endometrial receptivity in humans: protocol effects.** *Biology of reproduction* 2010, **82:**679-686.
11. Lu C-L, Yan Z-Q, Song X-L, Xu Y-Y, Zheng X-Y, Li R, Liu P, Feng H-L, Qiao J: **Effect of exogenous gonadotropin on the transcriptome of human granulosa cells and follicular fluid hormone profiles.** *Reproductive Biology and Endocrinology* 2019, **17:**49.
12. Sharma V, Whitehead M, Mason B, Pryse-Davies J, Ryder T, Dowsett M, Campbell S, Collins W: **Influence of superovulation on endometrial and embryonic development.** *Fertility and Sterility* 1990, **53:**822-829.
13. Kot K, Gibbons J, Ginther O: **A technique for intrafollicular injection in cattle: effects of hCG.** *Theriogenology* 1995, **44:**41-50.
14. da Silveira JC, Veeramachaneni DR, Winger QA, Carnevale EM, Bouma GJ: **Cell-secreted vesicles in equine ovarian follicular fluid contain miRNAs and proteins: a possible new form of cell communication within the ovarian follicle.** *Biology of reproduction* 2012, **86:**71, 71-10.
15. Sang Q, Yao Z, Wang H, Feng R, Wang H, Zhao X, Xing Q, Jin L, He L, Wu L: **Identification of microRNAs in human follicular fluid: characterization of microRNAs that govern steroidogenesis in vitro and are associated with polycystic ovary syndrome in vivo.** *The Journal of Clinical Endocrinology & Metabolism* 2013, **98:**3068-3079.
16. Hailay T, Hoelker M, Poirier M, Gebremedhn S, Rings F, Saeed-Zidane M, Salilew-Wondim D, Dauben C, Tholen E, Neuhoff C: **Extracellular vesicle-coupled miRNA profiles in follicular fluid of cows with divergent post-calving metabolic status.** *Scientific reports* 2019, **9:**1-14.
17. Di Pietro C: **Exosome-mediated communication in the ovarian follicle.** *Journal of assisted reproduction and genetics* 2016, **33:**303-311.
18. Tesfaye D, Hailay T, Salilew-Wondim D, Hoelker M, Bitseha S, Gebremedhn S: **Extracellular vesicle mediated molecular signaling in ovarian follicle: Implication for oocyte developmental competence.** *Theriogenology* 2020.
19. Dumesic DA, Meldrum DR, Katz-Jaffe MG, Krisher RL, Schoolcraft WB: **Oocyte environment: follicular fluid and cumulus cells are critical for oocyte health.** *Fertility and sterility* 2015, **103:**303-316.
20. Akbarzadeh A, Rezaei-Sadabady R, Davaran S, Woo Joo S, Zarghami N, Hanifehpour Y, Samiei M, Kouhi M, Nejati-Koshki K: **Liposome: Classification, preparation, and Applications.** *Nanoscale Research Letters* 2013, **8:**102.
21. Grijalva M, Vallejo-López MJ, Salazar L, Camacho J, Kumar B: **Cytotoxic and antiproliferative effects of nanomaterials on cancer cell lines: a review.** *Unraveling the Safety Profile of Nanoscale Particles and Materials: From Biomedical to Environmental Applications* 2018**:**63.
22. Feugang JM, Rhoads CE, Mustapha PA, Tardif S, Parrish JJ, Willard ST, Ryan PL: **Treatment of boar sperm with nanoparticles for improved fertility.** *Theriogenology* 2019, **137:**75-81.
23. Ferrazza RdA, Garcia HDM, Schmidt EMdS, Mihm Carmichael M, Souza FFd, Burchmore R, Sartori R, Eckersall PD, Ferreira JCP: **Quantitative proteomic profiling of bovine follicular fluid during follicle development.** *Biology of reproduction* 2017, **97:**835-849.
24. Fahiminiya S, Labas V, Roche S, Dacheux J-L, Gérard N: **Proteomic analysis of mare follicular fluid during late follicle development.** *Proteome science* 2011, **9:**54.
25. Dutra G, Ishak G, Pechanova O, Pechan T, Peterson D, Jacob J, Willard S, Ryan P, Gastal E, Feugang J: **Seasonal variation in equine follicular fluid proteome.** *Reproductive Biology and Endocrinology* 2019, **17:**29.

26. Paes VM, Liao SF, Figueiredo JR, Willard ST, Ryan PL, Feugang JM: **Proteome changes of porcine follicular fluid during follicle development.** *Journal of animal science and biotechnology* 2019, **10:**94.
27. Walter J, Huwiler F, Fortes C, Grossmann J, Roschitzki B, Hu J, Naegeli H, Laczko E, Bleul U: **Analysis of the equine "cumulome" reveals major metabolic aberrations after maturation in vitro.** *BMC genomics* 2019, **20:**588.
28. Ishak GM, Dutra GA, Gastal GD, Gastal MO, Feugang JM, Gastal EL: **Transition to the ovulatory season in mares: An investigation of antral follicle receptor gene expression in vivo.** *Molecular Reproduction and Development* 2019, **86:**1832-1845.
29. Ishak G, Bashir S, Dutra G, Gastal G, Gastal M, Cavinder C, Feugang J, Gastal E: **In vivo antral follicle wall biopsy: a new research technique to study ovarian function at the cellular and molecular levels.** *Reproductive Biology and Endocrinology* 2018, **16:**71.
30. Wang Q, He L, Fan D, Liang W, Fang J: **Improving the anti-inflammatory efficacy of dexamethasone in the treatment of rheumatoid arthritis with polymerized stealth liposomes as a delivery vehicle.** *Journal of Materials Chemistry B* 2020, **8:**1841-1851.
31. Ren H, He Y, Liang J, Cheng Z, Zhang M, Zhu Y, Hong C, Qin J, Xu X, Wang J: **Role of Liposome Size, Surface Charge, and PEGylation on Rheumatoid Arthritis Targeting Therapy.** *ACS Applied Materials & Interfaces* 2019, **11:**20304-20315.
32. Feugang JM, Youngblood RC, Greene JM, Willard ST, Ryan PL: **Self-illuminating quantum dots for non-invasive bioluminescence imaging of mammalian gametes.** *Journal of nanobiotechnology* 2015, **13:**38.
33. Ginther OJ, Siddiqui MAR, Beg MA: **Progesterone responses to intravenous and intrauterine infusions of prostaglandin F2 in mares.** *Reproduction, Fertility and Development* 2009, **21:**688-695.
34. Weber J, Causey R, Emmans E: **Induction of luteolysis in mares by ultrasound-guided intraluteal treatment with PGF2alpha.** *Theriogenology* 2001, **55:**1769-1776.
35. Ginther O, Gastal E, Gastal M, Bergfelt D, Baerwald A, Pierson R: **Comparative study of the dynamics of follicular waves in mares and women.** *Biology of reproduction* 2004, **71:**1195-1201.
36. Jha RK, Jha PK, Chaudhury K, Rana SVS, Guha SK: **An emerging interface between life science and nanotechnology: present status and prospects of reproductive healthcare aided by nano-biotechnology.** *Nano Reviews* 2014, **5:**10.3402/nano.v3405.22762.
37. Yáñez-Mó M, Siljander PR-M, Andreu Z, Bedina Zavec A, Borràs FE, Buzas EI, Buzas K, Casal E, Cappello F, Carvalho J: **Biological properties of extracellular vesicles and their physiological functions.** *Journal of extracellular vesicles* 2015, **4:**27066.
38. Stathopoulos G, Boulikas T: **Lipoplatin formulation review article.** *Journal of drug delivery* 2012, **2012**.
39. Carnevale E: **The mare model for follicular maturation and reproductive aging in the woman.** *Theriogenology* 2008, **69:**23-30.
40. Bashir ST, Baerwald AR, Gastal MO, Pierson RA, Gastal EL: **Follicle growth and endocrine dynamics in women with spontaneous luteinized unruptured follicles versus ovulation.** *Human Reproduction* 2018, **33:**1130-1140.
41. Quach N, Mock J, Scholpa N, Eggert M, Payre C, Lambeau G, Arnold R, Cummings B: **Role of the phospholipase A2 receptor in liposome drug delivery in prostate cancer cells.** *Molecular pharmaceutics* 2014, **11:**3443-3451.

42. Kamps JA, Morselt HW, Swart PJ, Meijer DK, Scherphof GL: **Massive targeting of liposomes, surface-modified with anionized albumins, to hepatic endothelial cells.** *Proceedings of the National Academy of Sciences* 1997, **94:**11681-11685.
43. Bartlett GR: **Phosphorus assay in column chromatography.** *Journal of Biological Chemistry* 1959, **234:**466-468.
44. Gastal E, Gastal M, Wiltbank M, Ginther O: **Follicle deviation and intrafollicular and systemic estradiol concentrations in mares.** *Biology of reproduction* 1999, **61:**31-39.

526 **Figure legends**
527
528 **Figure 1**. Liposome characterization through Malvern Zetasizer Nano ZS.
529 The Z-average diameter (**A**) and Zeta potential (**B**) parameters were measured in 3 replicates
530 (dilutions 1, 2, and 3). The insert is a TEM micrograph of liposome nanoparticles in monomer
531 (arrows) and aggregate formations.
532
533 **Figure 2**. Fluorescence imaging of liposome formulations using In Vivo Imaging System (IVIS).
534 Fluorescence imaging (480 nm excitation/570 nm emission) of 3 stock solutions (an average of
535 $1.9x10^{11} \pm 8.x10^{9}$ radiance efficiency; **A**) and the working solution (**B**) are shown. The blue box
536 surrounding the right panel (**B**) has a Phosphate-Buffered Saline solution (PBS) solution and
537 diluted liposome solution (23.1 µM; an average of $6.5x10^{10} \pm 8.x10^{9}$ radiance).
538
539 **Figure 3.** Fluorescence imaging of *in vitro* culture porcine follicles.
540 The micrograph (**A**) corresponds to fluorescence detected with In Vivo Imaging System (IVIS)
541 of pig follicles microinjected with 5 µl of Phosphate-Buffered Saline solution (PBS; upper
542 series), fluorescence liposomes (4.6 nmoles/follicle; middle series), and liposomal encapsulated
543 doxorubicin (10 µg/follicle; lower series) and cultured 24 h before imaging. All fluorescence
544 quantifications are shown in (**B**).
545
546 **Figure 4**. *In situ* fluorescence imaging of microinjected porcine follicles.
547 Following microinjection and 24 h culture of porcine follicles, follicles were fixed and subjected
548 to standard histology processing. Representative micrographs with sections of antral follicle
549 walls/layers injected with PBS (**A**, autofluorescence) or fluorescent liposomes (**B**, green color)
550 are shown. The green fluorescence is mainly located on the cell plasma membrane.
551 Representative micrographs with sections of antral follicles injected with non-fluorescent
552 liposomes loaded with doxorubicin are mainly located in the nuclei of follicle wall cells (**C, D**),
553 which colocalization with DAPI (blue) is highlighted with the insert in Micrograph D,
554 corresponding to fluorescence overlaid with visible light. Granulosa cells (GC), Theca interna
555 (TI), and Theca externa (TE) constitute the cell layers of the ovarian follicle wall.
556
557 **Figure 5**. Representative fluorescence imaging of equine follicle wall biopsies (FWB).
558 Biopsies were obtained from *in vivo* microinjected small (SF: n = 6) and large (LF: n = 5)
559 follicles. In parallel, FWB samples were harvested from Phosphate-Buffered Saline solution
560 (PBS)-injected follicles to serve as Control with a subset being *in vitro* labeled with comparable
561 fluorescence liposome concentrations. All FWB samples were imaged with the In Vivo Imaging
562 System (IVIS) and data (Radiant Efficiency) were quantified (mean ± sem). Letters indicate
563 significant differences (a, b, c; $P < 10^{-4}$). N = total number of samples analyzed.

564

565 **Figure 6**. Representative fluorescence imaging of equine follicular fluid (FF) following *in vivo*
566 labeling with fluorescence liposome nanoparticles.
567 The In Vivo Imaging System (IVIS) of FF collected from small and large follicles microinjected
568 with fluorescent liposomes is shown in **A** and **B**, respectively. The quantification of collected
569 fluorescence signals is plotted minus the values of FF originated from Phosphate-Buffered Saline
570 solution (PBS)-microinjected follicles that were considered as the background noise.
571 Fluorescence signal (Radiant Efficiency) data are mean (± SEM) and letters indicate a significant
572 difference (a, b; $P < 10^{-4}$). N = total number of samples analyzed.
573

574 **Figure 7**. Representative fluorescence imaging of *in vivo* labeled equine granulosa cells (GC).
575 The micrograph (left panel) shows tubes containing GC collected from follicles injected with
576 Phosphate-Buffered Saline solution (PBS) to serve as Control, and liposome-microinjected
577 follicles (**A**). Mean (± SEM) fluorescence data (Radiant Efficiency) of small (SF) and large (LF)
578 follicles are indicated (**B**). Letters denote significant differences (a, b, c; $P < P<10^{-5}$). N = total
579 number of samples analyzed.
580

581 **Figure 8.** *In vivo* fluorescence imaging of liposome binding to equine ovarian antral follicles.
582 Micrograph **A** showed a fragment of the follicle wall biopsy (FWB) of an antral follicle injected
583 with Phosphate-Buffered Saline solution (PBS). A representative sample of FWB harvested from
584 antral follicles injected with fluorescent liposomes are shown in Micrograph **B**. Granulosa cells
585 flushed from liposome injected antral follicles are shown in Micrographs **C and D**. The green
586 fluorescence detection of liposome was detected in the mural granulosa cells layers and the
587 major signal was located in the cells' plasma membrane (Insert in micrograph **B**), which is also
588 confirmed in Micrographs **C and D**. Nuclei are counterstained in blue with DAPI.
589

Figures

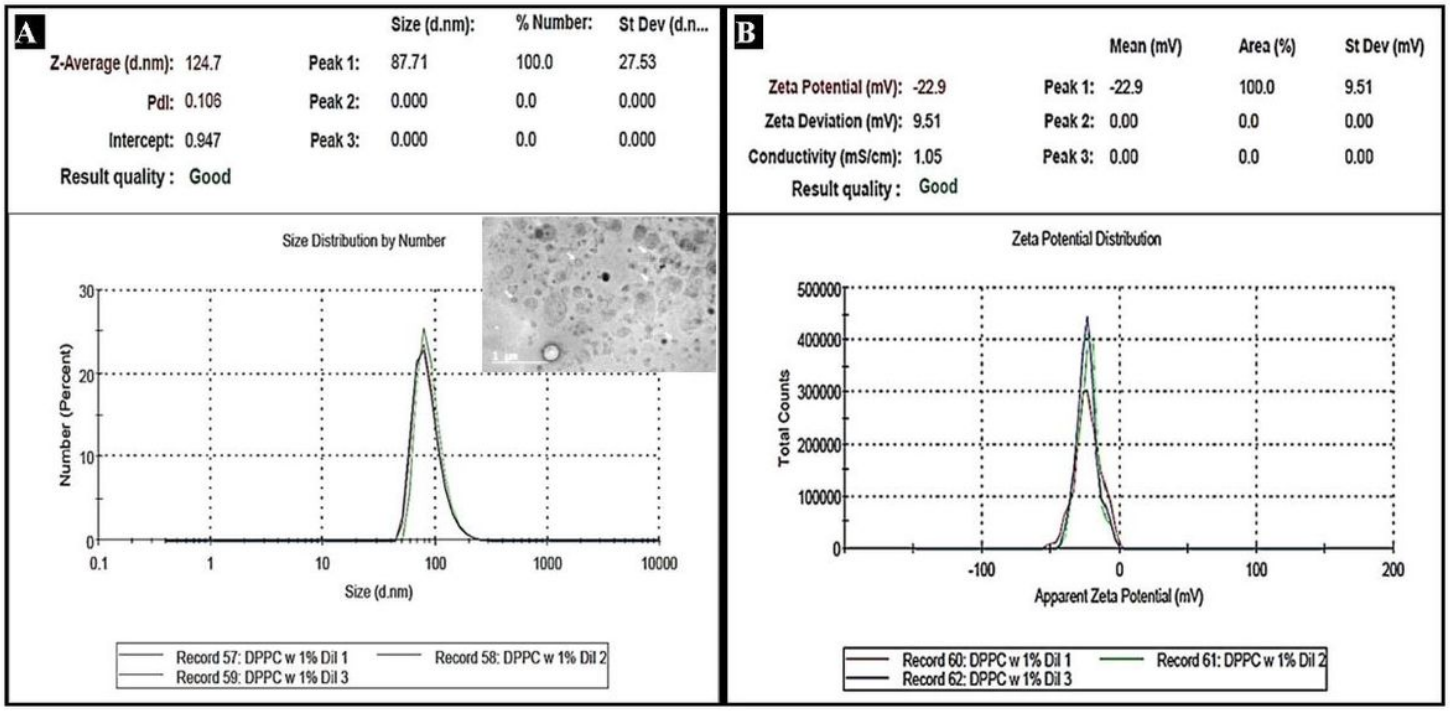

Figure 1

Liposome characterization through Malvern Zetasizer Nano ZS. The Z-average diameter (A) and Zeta potential (B) parameters were measured in 3 replicates (dilutions 1, 2, and 3). The insert is a TEM micrograph of liposome nanoparticles in monomer (arrows) and aggregate formations.

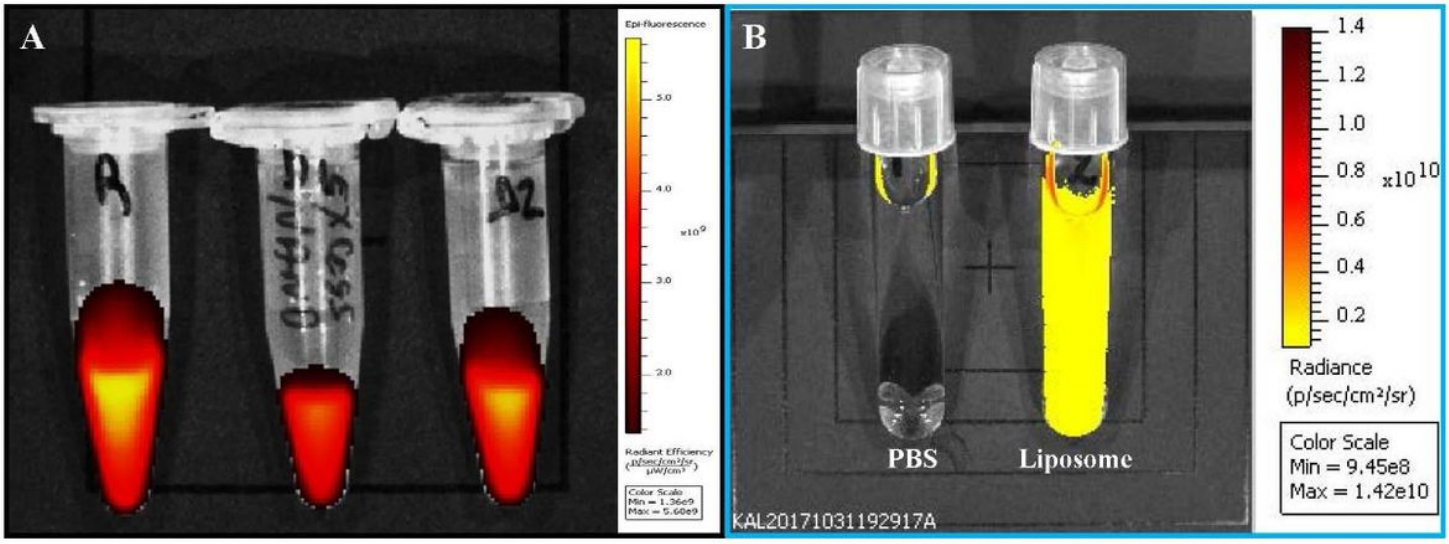

Figure 2

Fluorescence imaging of liposome formulations using In Vivo Imaging System (IVIS). Fluorescence imaging (480 nm excitation/570 nm emission) of 3 stock solutions (an average of 1.9x1011 ± 8.x109 radiance efficiency; A) and the working solution (B) are shown. The blue box surrounding the right panel (B) has a Phosphate-Buffered Saline solution (PBS) solution and diluted liposome solution (23.1 µM; an average of 6.5x1010 ± 8.x109 radiance).

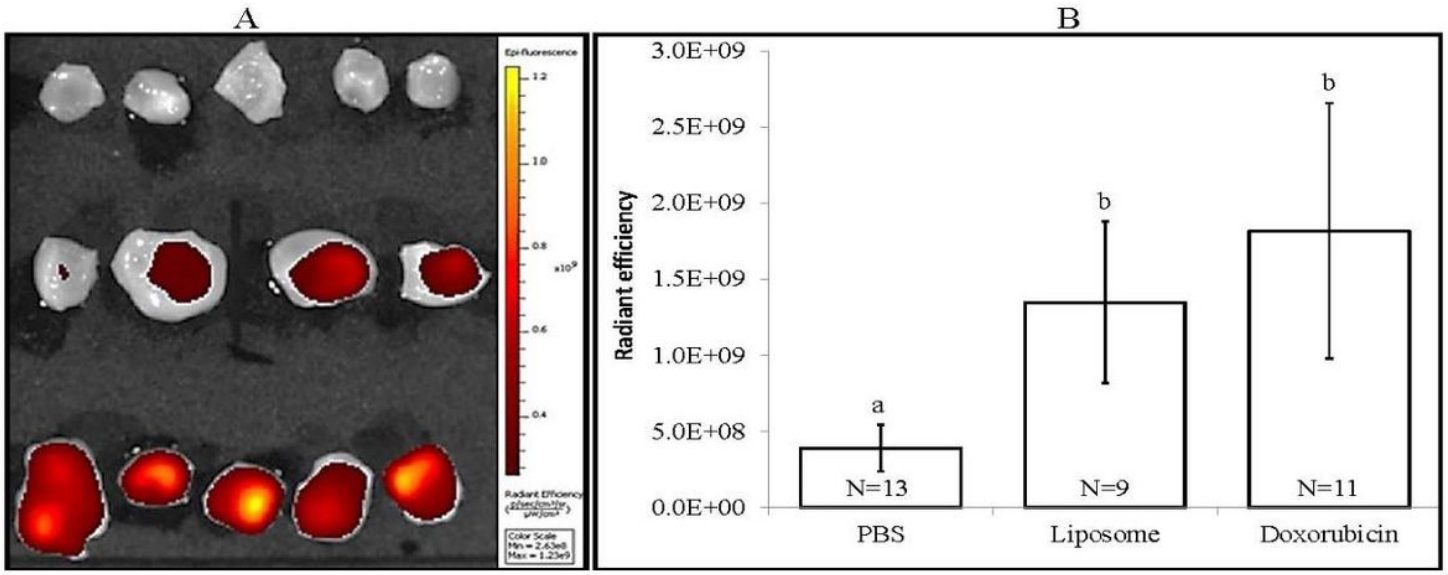

Figure 3

Fluorescence imaging of in vitro culture porcine follicles. The micrograph (A) corresponds to fluorescence detected with In Vivo Imaging System (IVIS) of pig follicles microinjected with 5 µl of Phosphate-Buffered Saline solution (PBS; upper series), fluorescence liposomes (4.6 nmoles/follicle; middle series), and liposomal encapsulated doxorubicin (10 µg/follicle; lower series) and cultured 24 h before imaging. All fluorescence quantifications are shown in (B).

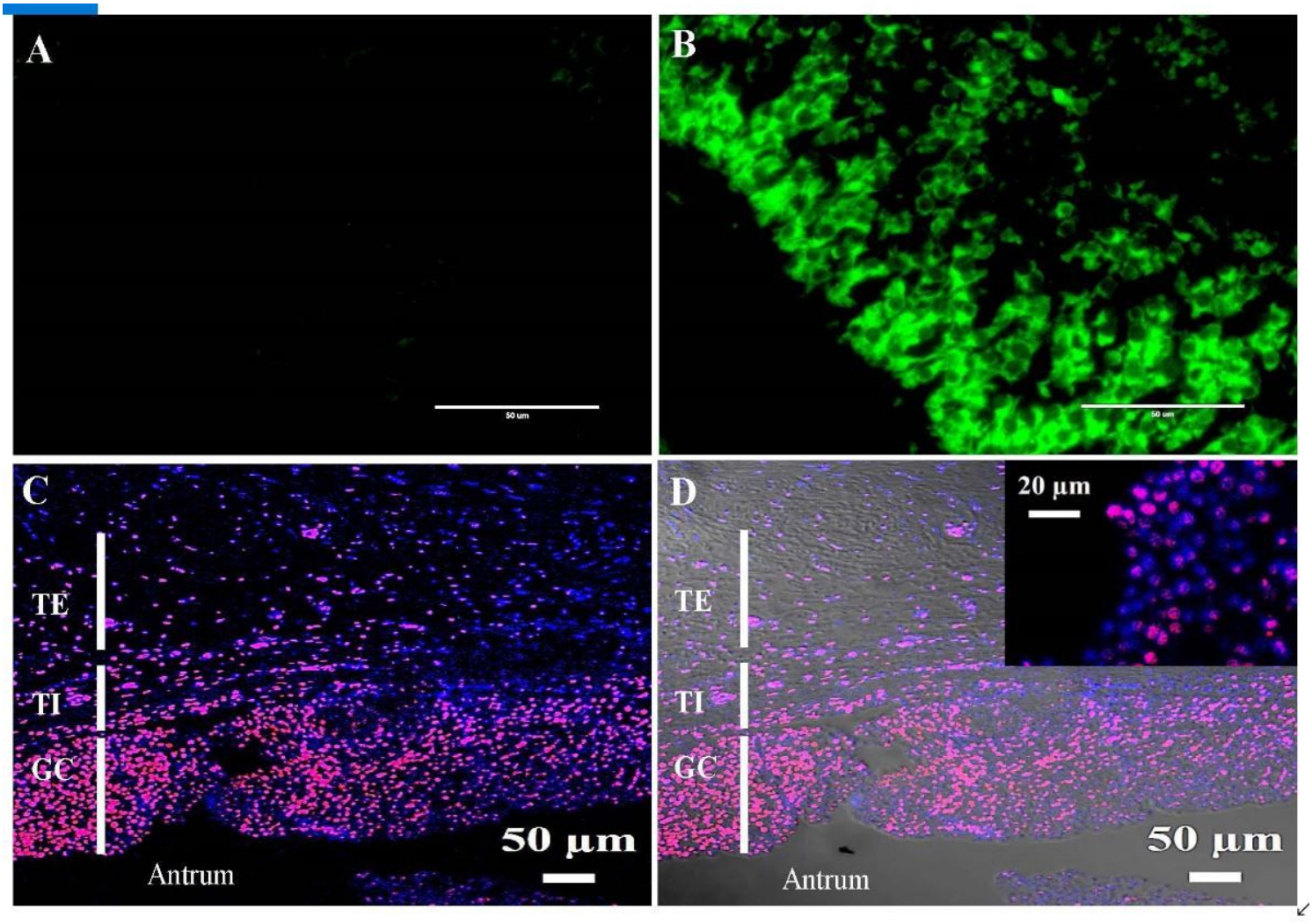

Figure 4

In situ fluorescence imaging of microinjected porcine follicles. Following microinjection and 24 h culture of porcine follicles, follicles were fixed and subjected to standard histology processing. Representative micrographs with sections of antral follicle walls/layers injected with PBS (A, autofluorescence) or fluorescent liposomes (B, green color) are shown. The green fluorescence is mainly located on the cell plasma membrane. Representative micrographs with sections of antral follicles injected with non-fluorescent liposomes loaded with doxorubicin are mainly located in the nuclei of follicle wall cells (C, D), which colocalization with DAPI (blue) is highlighted with the insert in Micrograph D, corresponding to fluorescence overlaid with visible light. Granulosa cells (GC), Theca interna (TI), and Theca externa (TE) constitute the cell layers of the ovarian follicle wall.

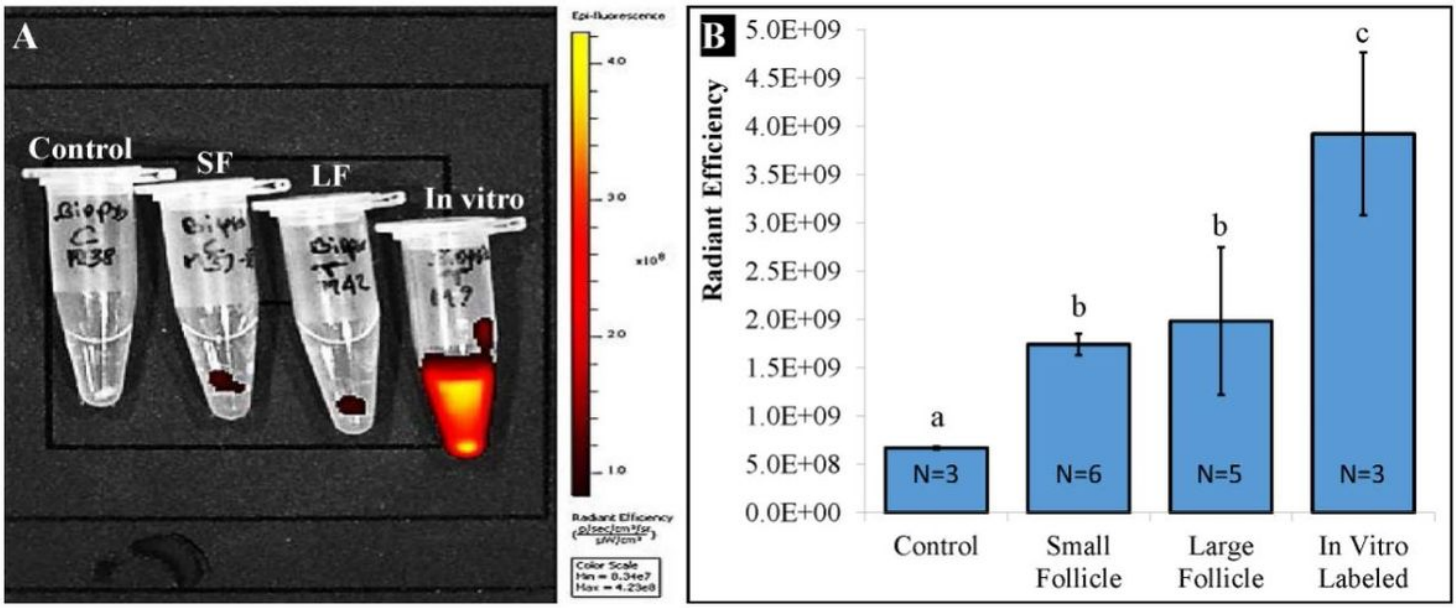

Figure 5

Representative fluorescence imaging of equine follicle wall biopsies (FWB). Biopsies were obtained from in vivo microinjected small (SF: n = 6) and large (LF: n = 5) follicles. In parallel, FWB samples were harvested from Phosphate-Buffered Saline solution (PBS)-injected follicles to serve as Control with a subset being in vitro labeled with comparable fluorescence liposome concentrations. All FWB samples were imaged with the In Vivo Imaging System (IVIS) and data (Radiant Efficiency) were quantified (mean ± sem). Letters indicate significant differences (a, b, c; P < 10–4). N = total number of samples analyzed.

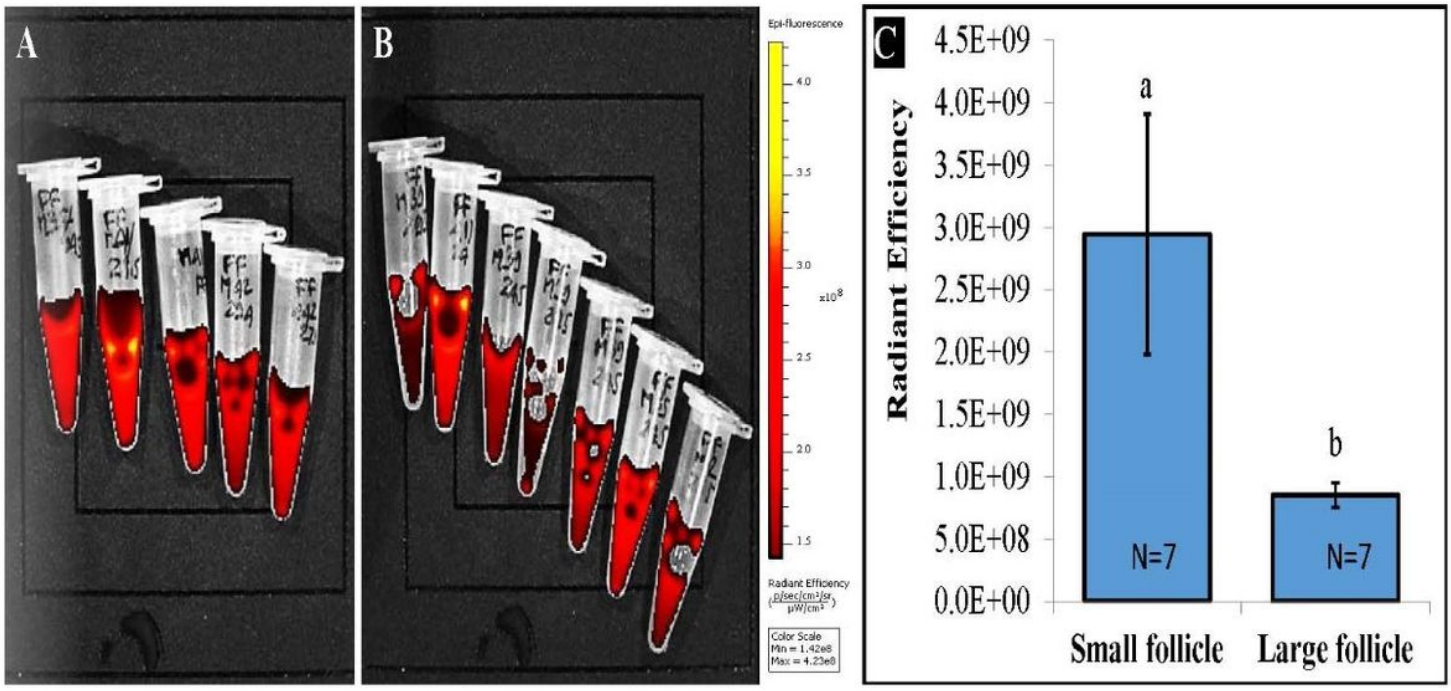

Figure 6

Representative fluorescence imaging of equine follicular fluid (FF) following in vivo labeling with fluorescence liposome nanoparticles. The In Vivo Imaging System (IVIS) of FF collected from small and large follicles microinjected with fluorescent liposomes is shown in A and B, respectively. The quantification of collected fluorescence signals is plotted minus the values of FF originated from Phosphate-Buffered Saline solution (PBS)-microinjected follicles that were considered as the background noise. Fluorescence signal (Radiant Efficiency) data are mean (± SEM) and letters indicate a significant difference (a, b; P < 10–4). N = total number of samples analyzed.

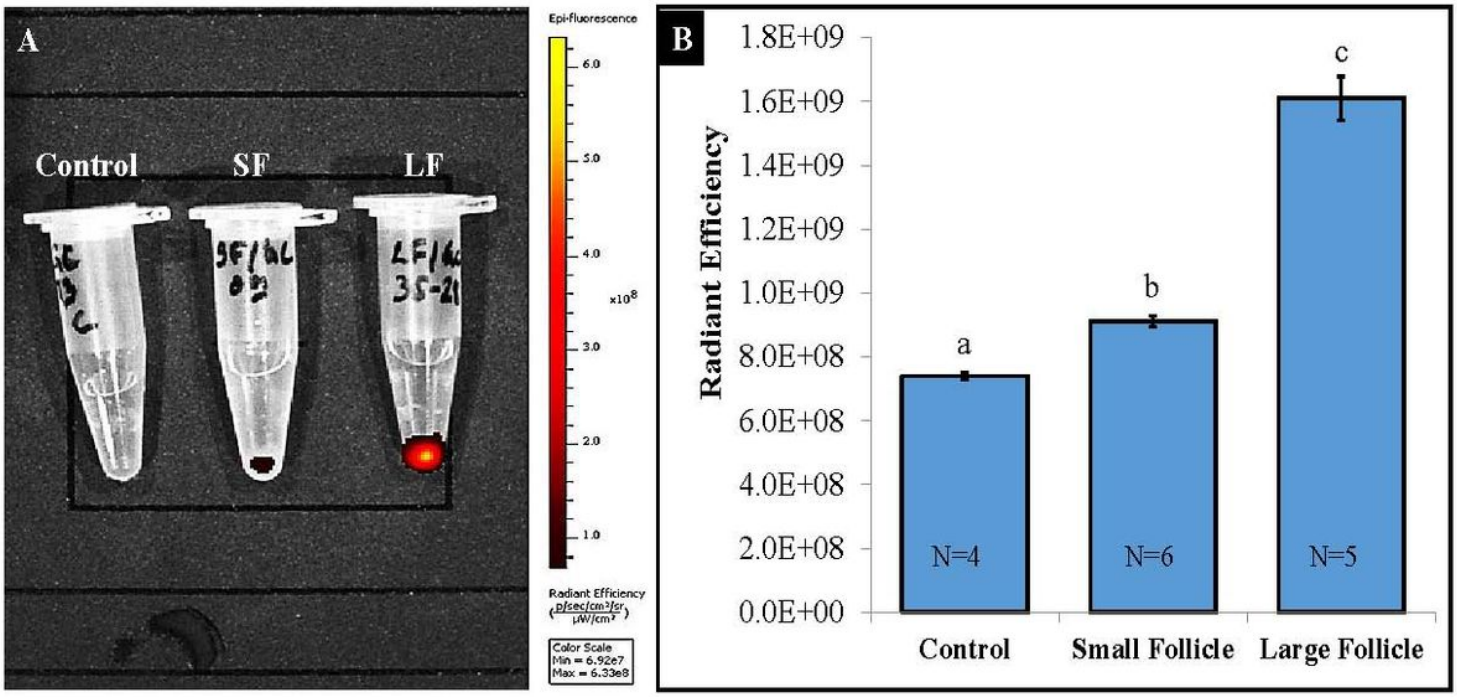

Figure 7

Representative fluorescence imaging of in vivo labeled equine granulosa cells (GC). The micrograph (left panel) shows tubes containing GC collected from follicles injected with Phosphate-Buffered Saline solution (PBS) to serve as Control, and liposome-microinjected follicles (A). Mean (± SEM) fluorescence data (Radiant Efficiency) of small (SF) and large (LF) follicles are indicated (B). Letters denote significant differences (a, b, c; P < P<10–5). N = total number of samples analyzed.

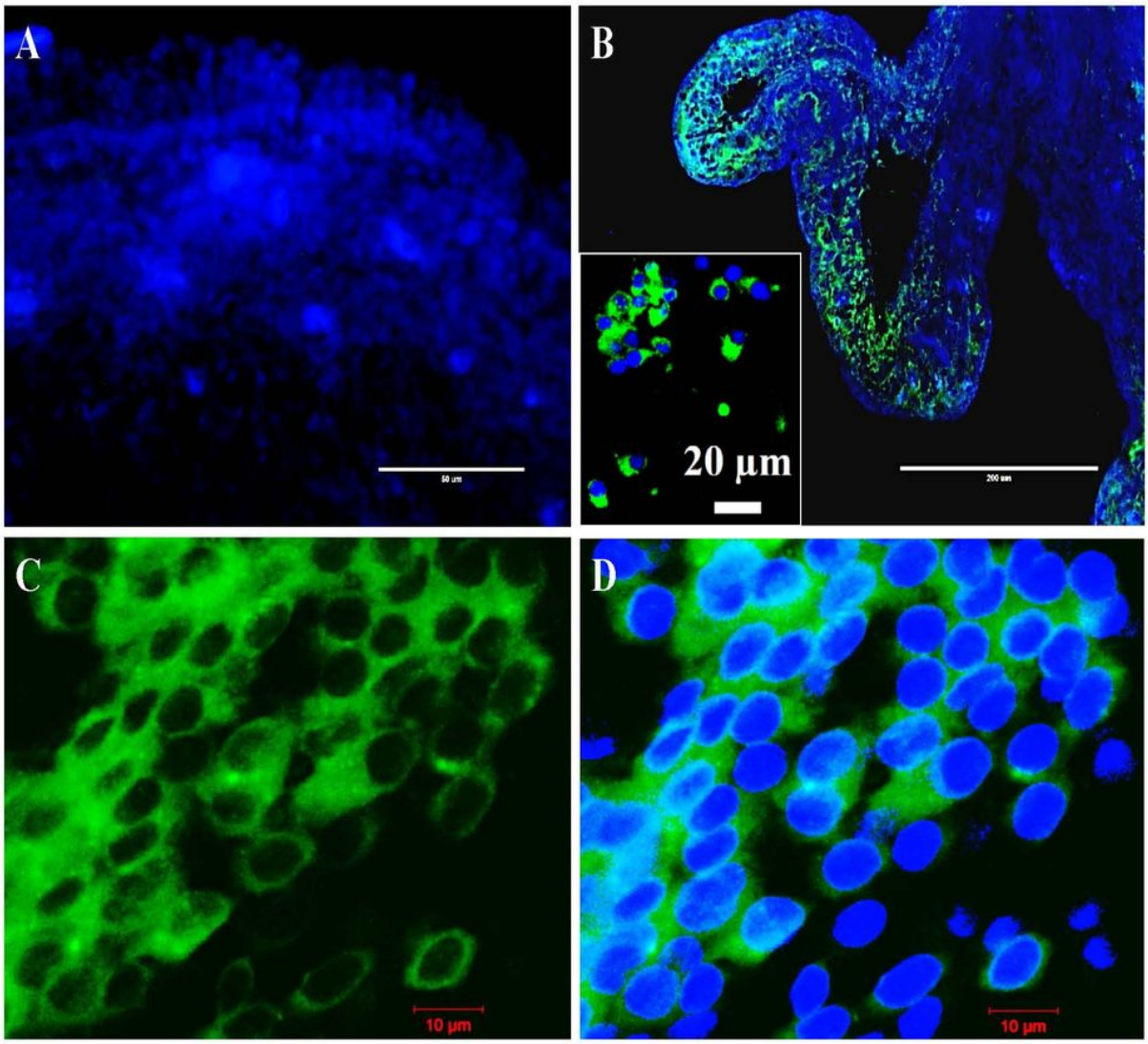

Figure 8

In vivo fluorescence imaging of liposome binding to equine ovarian antral follicles. Micrograph A showed a fragment of the follicle wall biopsy (FWB) of an antral follicle injected with Phosphate-Buffered Saline solution (PBS). A representative sample of FWB harvested from antral follicles injected with fluorescent liposomes are shown in Micrograph B. Granulosa cells flushed from liposome injected antral follicles are shown in Micrographs C and D. The green fluorescence detection of liposome was detected in the mural granulosa cells layers and the major signal was located in the cells' plasma membrane (Insert in micrograph B), which is also confirmed in Micrographs C and D. Nuclei are counterstained in blue with DAPI.